J|A|C|S
ARTICLES
Published on Web 11/24/2004

Temperature-Dependent Behavior of a Symmetric Long-Chain Bolaamphiphile with Phosphocholine Headgroups in Water: From Hydrogel to Nanoparticles

Karen Köhler,[†,‡] Günter Förster,[†] Anton Hauser,[†] Bodo Dobner,[§] Ulrich F. Heiser,[§] Friederike Ziethe,[§] Walter Richter,[∥] Frank Steiniger,[∥] Markus Drechsler,[⊥,+] Heiko Stettin,[&] and Alfred Blume*[,†]

Contribution from the MLU Halle-Wittenberg, Institut für Physikalische Chemie, Mühlpforte 1, 06108 Halle/Saale, Germany, FSU Jena, Institut für Ultrastrukturforschung, Ziegelmühlenweg 1, 07740 Jena, Germany, FSU Jena, Institut für Pharmazie, Philosophenweg 14, 07743 Jena, Germany, and Physica Messtechnik GmbH, Helmuth-Hirth-Strasse 6, 73760 Ostfildern, Germany

Received June 11, 2004; E-mail: blume@chemie.uni-halle.de

Abstract: The temperature-dependent self-assembly of the single-chain bolaamphiphile dotriacontan-1,1′-diyl-bis[2-(trimethylammonio)ethyl phosphate] (PC−C32−PC) was investigated by transmission electron microscopy (TEM), differential scanning calorimetry (DSC), Fourier transform infrared spectroscopy (FT-IR), X-ray scattering, rheological measurements, and dynamic light scattering (DLS). At room temperature this compound, in which two phosphocholine headgroups are connected by a C_{32} alkyl chain, proved to be capable of gelling water very efficiently by forming a dense network of nanofibers (Köhler et al. *Angew. Chem., Int. Ed.* **2004**, *43*, 245). A specific feature of this self-assembly process is that it is not driven by hydrogen bonds but solely by hydrophobic interactions of the long alkyl chains. The nanofibers have a thickness of roughly the molecular length and show a helical superstructure. A model for the molecular structure of the fibrils which considers the extreme constitution of the bolaamphiphile is proposed. Upon heating the suspensions three different phase transitions can be detected. Above 49 °C, the temperature of the main transition where the alkyl chains become "fluid", a clear low-viscosity solution is obtained due to a breakdown of the fibrils into smaller aggregates. Through mechanical stress the gel structure can be destroyed as well, indicating a low stability of these fibers. The gel formation is reversible, but as a drastic rearrangement of the molecules takes place, metastable states occur.

Introduction

Molecular self-assembly has attracted considerable attention in generating new nonbiological well-defined structures with dimensions of 1−100 nm which have great potential for the development of advanced materials.[1] The noncovalent interactions that lead to the formation of molecular order in these aggregates include hydrogen bonds, van der Waals forces, hydrophobic interactions, electrostatic forces, dipole−dipole interactions, and $\pi-\pi$-stacking. The structure of molecules which are capable of self-assembly turns out to be manifold. Often compounds with structural elements of biological model molecules are synthesized to take advantage of their intermolecular interactions. Specific examples for such residues are nucleosides,[2] sugars,[3] and amino acids[4] or peptides[5] which can form strong hydrogen bonds leading to intermolecular aggregation. In this respect, low-molecular gelling agents are a special area of interest. They form a three-dimensional network within the solvent so that it cannot flow freely. The immobilization of 10^5 liquid molecules induced by only one gelator molecule is not uncommon for organogels formed through self-assembly.[6−9] Most of the known aqueous gels consist of macromolecules such as proteins or other polymers.[10−13] However, there are only a

[†] MLU Halle-Wittenberg, Institut für Physikalische Chemie.
[‡] Current address: Max-Planck Institute of Colloids and Interfaces, 14424 Golm/Potsdam, Germany.
[§] MLU Halle-Wittenberg, Institut für Pharmazeutische Chemie.
[∥] FSU Jena, Institut für Ultrastrukturforschung.
[⊥] FSU Jena, Institut für Pharmazie.
[+] Current address: University of Bayreuth, Macromolecular Chemistry II, 95440 Bayreuth, Germany.
[&] Physica Messtechnik GmbH.

(1) Whitesides, G. M.; Mathias, J. P.; Seto, C. T. *Science* **1991**, *254*, 1312−1319.
(2) Itojima, Y.; Ogawa, Y.; Tsuno, K.; Handa, N.; Yanagawa, H. *Biochemistry* **1992**, *31*, 4757−4765.
(3) Masuda, M.; Vill, V.; Shimizu, T. *J. Am. Chem. Soc.* **2000**, *122*, 12327−12333.
(4) Song, J.; Cheng, Q.; Kopta, S.; Stevens, R. C. *J. Am. Chem. Soc.* **2001**, *123*, 3205−3213.
(5) Hartgerink, J. D.; Beniash, E.; Stupp, S. I. *PNAS* **2002**, *99*, 5133−5138.
(6) Hanabusa, K.; Shimura, K.; Hirose, K.; Kimura, M.; Shirai, H. *Chem. Lett.* **1996**, 885−886.
(7) Murdan, S.; Gregoriadis, G.; Florence, A. T. *J. Pharm. Sci.* **1999**, *88*, 608−614.
(8) Terech, P.; Pasquier, D.; Bordas, V.; Rossat, C. *Langmuir* **2000**, *16*, 4485−4494.
(9) Placin, F.; Desvergne, J.-P.; Belin, C.; Buffeteau, T.; Desbat, B.; Ducasse, L.; Lassègues, J.-C. *Langmuir* **2003**, *19*, 4563−4572.
(10) Chen, G. H.; Hoffman, A. S. *Nature* **1995**, *373*, 49−52.
(11) Yoshida, R.; Uchida, K.; Kaneko, Y.; Sakai, K.; Kikuchi, A.; Sakurai, Y.; Okano, T. *Nature* **1995**, *374*, 240−242.
(12) Wang, C.; Stewart, R. J.; Kopeček, J. *Nature* **1999**, *397*, 417−420.

10.1021/ja046537k CCC: $27.50

few reports on hydrogels which are composed of low molecular weight compounds so far.[14−19] These hydrogelators offer the advantage of easily controllable gel properties, e.g., by changing the temperature, pH, or mechanical agitation of the suspension. Due to their remarkable properties, low molecular weight gelators could find application in the fields of cosmetics, drug delivery, or photographic industry as stimuli-responsive materials.

We are interested in self-assembly properties of long-chain bolaamphiphiles. Bolaamphiphiles or bolaform amphiphiles consisting of two hydrophilic headgroups connected by a hydrophobic core[20] can be assumed as model compounds for bolalipids from archaebacterial membranes.[21−23] The aggregation morphologies of bolaamphiphiles are as variable as their molecular structures.[24,25] Besides vesicles[20,26] and lamellae,[27] disks,[28] rods,[29] tubules,[29] ribbons, and fibers[30] in the nano- and micrometer range could be observed. Some chiral bolaamphiphiles derived from biomolecules even form chiral superstructures such as helices.[31] There are only a few reports on bolaamphiphilic hydrogelators so far. Among these compounds are dendritic arborols[32,33] with several hydroxyl groups, nucleotide-appended bolaamphiphiles,[34] bis-urea dicarboxylic acids,[35,36] and aldopyranoside-based bolaamphiphiles.[37] As mentioned above for low-molecular weight hydrogelators, the self-assembly process is mainly driven by formation of strong hydrogen bonds.

We present here a detailed investigation of the temperature-dependent aggregation properties of dotriacontan-1,1′-diyl-bis-[2-(trimethylammonio)ethyl phosphate] (PC−C32−PC) by means of transmission electron microscopy (TEM), differential scanning calorimetry (DSC), Fourier transform infrared spectroscopy (FT-IR), X-ray scattering, rheological measurements, and dynamic light scattering (DLS). PC−C32−PC has a C_{32} alkyl chain that connects two polar phosphocholine headgroups. Dispersed in water, it shows a new self-assembly model because this process leading to a hydrogel seems to be exclusively driven by hydrophobic effects.[38] The similarly built compound with a C_{22} alkyl chain docosan-1,1′-diyl-bis[2-(trimethylammonio)ethyl phosphate] (Irlbacholin) is found in the plants *Irlbachia alata* and *Anthocleista djalonensis*.[39] This agent is used in plant medicine, being affective against fungi *Candida albicans*, *Cryptococcus neoformans*, *Aspergillus fumigatos*, and *Trichophyton rubrum*.[40]

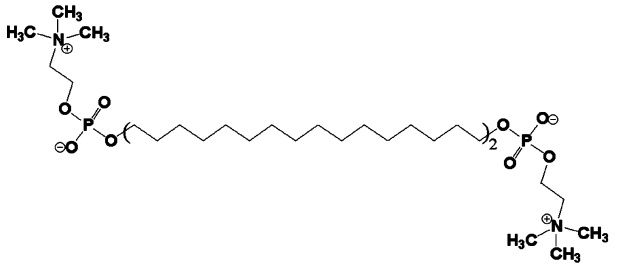

Figure 1. Chemical structure of the bolaamphiphile PC−C32−PC consisting of two bulky phosphocholine headgroups connected by a C_{32} alkyl chain.

Results and Discussion

Aggregation Behavior at Room Temperature. The bolaamphiphile PC−C32−PC has a chemical structure (Figure 1) with a large difference in space requirement between the headgroup and the alkyl chain. This bolalipid exhibits excellent properties as a hydrogelator at room temperature. Clear suspensions of different lipid concentrations were prepared by heating PC−C32−PC in water above the gel temperature. Already at concentrations of 1 mg mL^{-1} PC−C32−PC the complete gelation of water is obtained, so that the vial can be turned upside down without downward flow of the almost transparent gel. An increase of the bolaamphiphile concentration decreases the gelation time remarkably. At a concentration of 5 mg mL^{-1} the suspension gelatinizes immediately, whereas at 1 mg mL^{-1} it takes approximately 1 h. The gel structure is stable for at least several months. Through mechanical stress and at temperatures above 50 °C, the gel character disappears and a clear isotropic fluid is obtained. Upon gradual cooling the gel is reformed again. Therefore, the bolaamphiphile−water system can be regarded as a thermoreversible hydrogelator. At a concentration of 1 mg of PC−C32−PC per milliliter of water, approximately 45 000 bound solvent molecules per bipolar lipid molecule are immobilized.[38]

To determine the exact structure of the network, we investigated diluted suspensions of PC−C32−PC (0.3 mg mL^{-1}) by means of transmission electron microscopy using staining with uranyl acetate. The images show a dense three-dimensional

(13) Lee, K. Y.; Mooney, D. J. *Chem. Rev.* **2001**, *101*, 1869−1879.
(14) Fuhrhop, J.-H.; Boettcher, C. *J. Am. Chem. Soc.* **1990**, *112*, 1768−1776.
(15) Oda, R.; Huc, I.; Candau, S. J. *Angew. Chem., Int. Ed.* **1998**, *37*, 2689−2691.
(16) Bhattacharya, S.; Acharya, S. N. G. *Chem. Mater.* **1999**, *11*, 3121−3132.
(17) Menger, F. M.; Caran, K. L. *J. Am. Chem. Soc.* **2000**, *122*, 11679−11691.
(18) Marmillon, C.; Gauffre, F.; Gulik-Krzywicki, T.; Loup, C.; Caminade, A.-M.; Majoral, J.-P.; Vors, J.-P.; Rump, E. *Angew. Chem., Int. Ed.* **2001**, *40*, 2626−2629.
(19) Kiyonaka, S.; Shinkai, S.; Hamachi, I. *Chem. Eur. J.* **2003**, *9*, 976−983.
(20) Fuhrhop, J.-H.; David, H.-H.; Mathieu, J.; Liman, U.; Winter, H.-J.; Boekema, E. *J. Am. Chem. Soc.* **1986**, *108*, 1785−1791.
(21) Danson, M. J.; Hough, D. W.; Lunt, G. G. *The Archaebacteria: Biochemistry and Biotechnology;* Portland Press: London, 1992.
(22) Kates, M.; Kushner, D. J.; Matheson, A. T. *The Biochemistry of Archae (Archaebacteria);* Elsevier: Amsterdam, 1993.
(23) Robb, F. T.; Place, A. R.; Sowers, K. R.; Schreier, H. J.; DasSarina, S.; Fleischmann, E. M. *Archae−A laboratory manual*; Cold Spring Harbor Laboratory Press: New York, 1995.
(24) Sirieix, J.; Lauth-de Viguerie, N.; Riviere, M.; Lattes, A. *New J. Chem.* **2000**, *24*, 1043−1048.
(25) Shimizu, T. *Macromol. Rapid Commun.* **2002**, *23*, 311−331.
(26) Sirieix, J.; Lauth-de Viguerie, N.; Riviere, M.; Lattes, A. *Langmuir* **2000**, *16*, 9221−9224.
(27) Thompson, D. H.; Wong, K. F.; Humphry-Baker, R.; Wheeler, J. J.; Kim, J.-M.; Rananavare, S. B. *J. Am. Chem. Soc.* **1992**, *114*, 9035−9042.
(28) Guilbot, J.; Benvegnu, T.; Legros, N.; Plusquellec, D. *Langmuir* **2001**, *17*, 613−618.
(29) Fuhrhop, J.-H.; Spiroski, D.; Boettcher, C. *J. Am. Chem. Soc.* **1993**, *115*, 1600−1601.
(30) Shimizu, T.; Iwaura, R.; Masuda, M.; Hanada, T.; Yase, K. *J. Am. Chem. Soc.* **2001**, *123*, 5947−5955.
(31) Nakazawa, I.; Masuda, M.; Okada, Y.; Hanada, T.; Yase, K.; Asai, M.; Shimizu, T. *Langmuir* **1999**, *15*, 4757−4764.
(32) Newkome, G. R.; Baker, G. R.; Arai, S.; Saunders, M. J.; Russo, P. S.; Theriot, K. J.; Moorefield, C. N.; Rogers, L. E.; Miller, J. E.; Lieux, T. R.; Murray, M. E.; Phillips, B.; Pascal, L. *J. Am. Chem. Soc.* **1990**, *112*, 8458−8465.
(33) Engelhardt, T.-P.; Belkoura, L.; Woermann, D. *Ber. Bunsen-Ges. Phys. Chem.* **1996**, *100*, 1064−1072.
(34) Iwaura, I.; Yoshida, K.; Masuda, M.; Yase, K.; Shimizu, T. *Chem. Mater.* **2002**, *14*, 3047−3053.
(35) Estroff, L. A.; Hamilton, A. D. *Angew. Chem., Int. Ed.* **2000**, *39*, 3447−3450.
(36) Estroff, L. A.; Leiserowitz, L.; Addadi, L.; Weiner, S.; Hamilton, A. D. *Adv. Mater.* **2003**, *15*, 38−42.
(37) Jung, H. J.; Shinkai, S.; Shimizu, T. *Chem. Eur. J.* **2002**, *8*, 2684−2690.
(38) Köhler, K.; Förster, G.; Hauser, A.; Dobner, B.; Heiser, U. F.; Ziethe, F.; Richter, W.; Steiniger, F.; Drechsler, M.; Stettin, H.; Blume, A. *Angew. Chem., Int. Ed.* **2004**, *43*, 245−247.
(39) Bierer, D. E.; Gerber, R. E.; Jolad, S. D.; Ubillas, R. P.; Randle, J.; Nauka, E.; Latour, J.; Dener, J. M.; Fort, D. M.; Kuo, J. E.; Inman, W. D.; Dubenko, L. G.; Ayala, F.; Ozioko, A.; Obialor, C.; Elisabetsky, E.; Carlson, T.; Truong, T. V.; Bruening, R. C. *J. Org. Chem.* **1995**, *60*, 7022−7026.
(40) Lu, Q.; Ubillas, R. P.; Zhou, Y.; Dubenko, L. G.; Dener, J. M.; Litvak, J.; Phuan, P.-W.; Flores, M.; Ye, Z.; Gerber, R. E.; Truong, T.; Bierer, D. E. *J. Nat. Prod.* **1999**, *62*, 824−828.

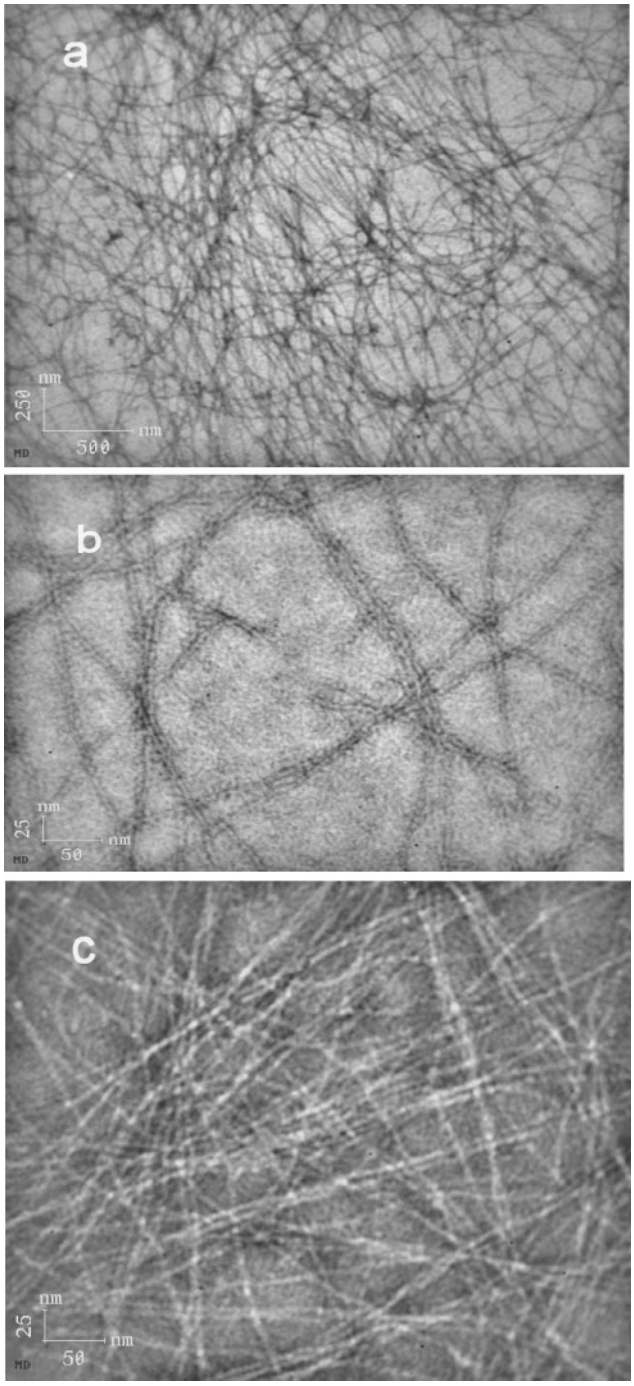

Figure 2. TEM images of an aqueous uranyl acetate stained suspension of 0.3 mg mL^{-1} PC−C32−PC at room temperature. (a) Sample at low uranyl acetate concentration. Fibers are positively stained by uranyl acetate. (b) Sample at larger magnification. The fibers seem to be structured. (c) Sample with higher uranyl acetate concentration. In the lower layers the fibers seem to arrange in a parallel fashion.

network of fibrils which all have the same thickness of approximately 6−7 nm and a length of several micrometers (Figure 2a and b). The thickness corresponds roughly to the length of the extended PC−C32−PC molecule; however, it is slightly larger due to the positive staining caused by the binding of the uranyl ions to the phosphocholine headgroups. The fibers adopt mainly an extended conformation with only a few bends, indicating a slight flexibility of these aggregate structures.

In Figure 2c it can be seen that at higher local uranyl acetate concentration the background is dark due to the negative staining

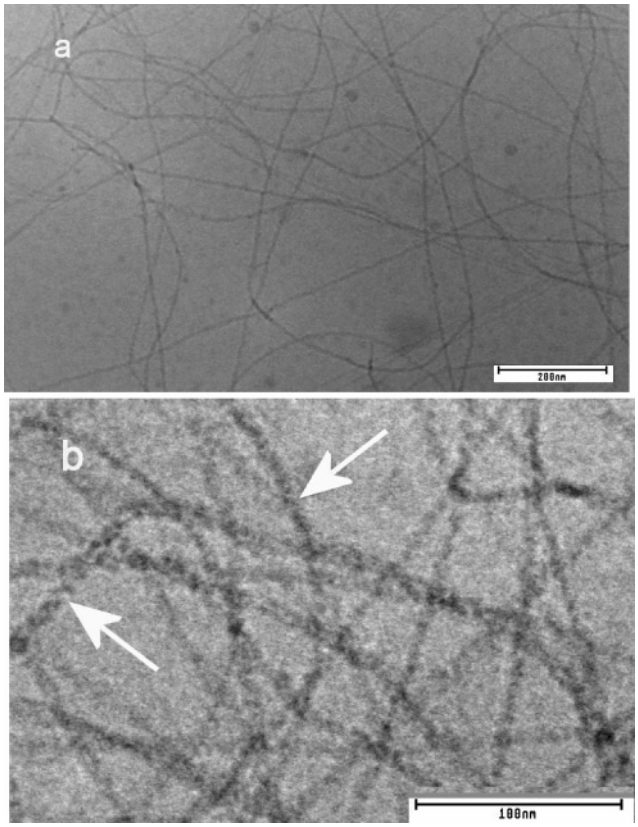

Figure 3. Cryoelectron transmission micrographs of PC−C32−PC fibers at two different magnifications. The arrows point to an apparent helical structuring of the fibers.

effect caused by the higher uranyl acetate concentration and the fibers seem thinner and seem to orient parallel to each other, particularly on the surface of the grid.

To exclude the influence of the staining agent on the aggregate formation and to be sure that no changes occur during drying, cryotransmission electron microscopy was additionally used to image the fibers. With this technique the same dense network of fibrils can be observed (Figure 3a). Due to the better resolution, since no staining agent is necessary, a helical structuring seems to be discernible (Figure 3b). Because the resolution of the microscope is limited, the helical arrangement cannot be seen very clearly and also not on every fibril.

The pitch of these helices is approximately 5.5 nm, and the angle to the helix axis is about 55°. Because of the resolution problem, we are not able to obtain quantitative statistics about the overall chirality but could find both kinds of handedness. PC−C32−PC does not have a chiral center, so that equal amounts of right-handed and left-handed helices must be formed to give a racemic mixture. The phenomenon that chiral structures can occur being built up by nonchiral molecules is known as spontaneous symmetry breaking. To date it has been observed in various assemblies such as liquid crystals,[41] Langmuir−Blodgett films of calcium arachidate,[42] and sodium chlorate crystals.[43] In these cases the symmetry breaking is explained by packing restrictions between different parts of the molecules

(41) Jákli, A.; Nair, G. G.; Lee, C. K.; Sun, R.; Chien, L. C. *Phys. Rev. E* **2001**, *63*, 061710/1−5.
(42) Viswanathan, R.; Zasadzinski, J. A.; Schwartz, D. K. *Nature* **1994**, *368*, 440−443.
(43) Kondepudi, D. K.; Kaufman, R. J.; Singh, N. *Science* **1990**, *250*, 975−977.

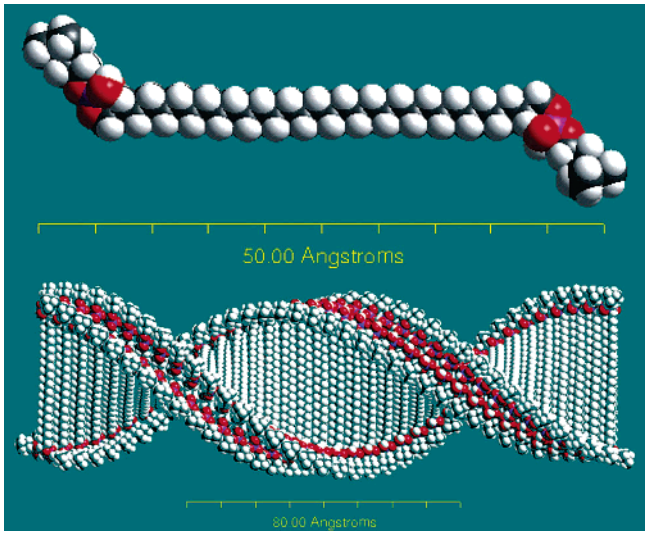

Figure 4. Proposed helical arrangement of PC−C32−PC molecules within the nanofibers with molecules arranged side by side but twisted relative to each other because of the bulky headgroups.

or by the interplay of surface and volume effects. It is assumed that the inversion symmetry is broken at the surface of the structures. In our PC−C32−PC/water system packing restrictions also play an important role owing to the larger space requirements of the phosphocholine headgroup in comparison to the small cross-sectional area of the alkyl chain. Consequently, monolayer structures with parallel oriented bolaform molecules are not sufficiently stabilized by the hydrophobic effect since the lipophilic chains cannot come close enough to each other. Strong interactions between the bolaamphiphile molecules via hydrogen bonds are not possible because PC−C32−PC does not have any hydrogen atoms functioning as possible hydrogen-bond donors when the bolalipid is suspended at neutral pH. Therefore, the molecular aggregation of PC−C32−PC to build up nanofibrils can only be driven by hydrophobic interactions between the alkyl chains. The extreme molecular structure of PC−C32−PC with its two large headgroups and its long alkyl chain with small cross-sectional area has to be taken into account for a suggestion of a possible fiber structure. The alignment of the bolaamphiphile molecules within the helical fibrils could be as follows: The molecules are in an extended conformation and arranged next to each other. On account to the bulky phosphocholine headgroups, a parallel packing of the molecules with a stabilizing interaction of the hydrophobic chains is not possible. To maximize the interaction of the chains of adjacent molecules, they could be slightly twisted relative to each other, so that the greatest possible approach of the alkyl chains is reached (Figure 4). In this model we assume extended molecules whose alkyl chains are in an all-trans conformation. This was confirmed by IR spectroscopy (see below). Molecules arranged in that way lead to a helical cylindrical structure with a diameter that corresponds to the molecular length as seen in the TEM images. The model shown in Figure 4 is built up from two molecules lying side by side, the axis of the molecules being slightly twisted in the next layer on top. The handedness of the helix is determined by the first two or more aggregating molecules, so left-handed as well as right-handed helices should be equally probable. It is likely that not only two but also several molecules are oriented more or less parallel to each other as well as perpendicular to the helix

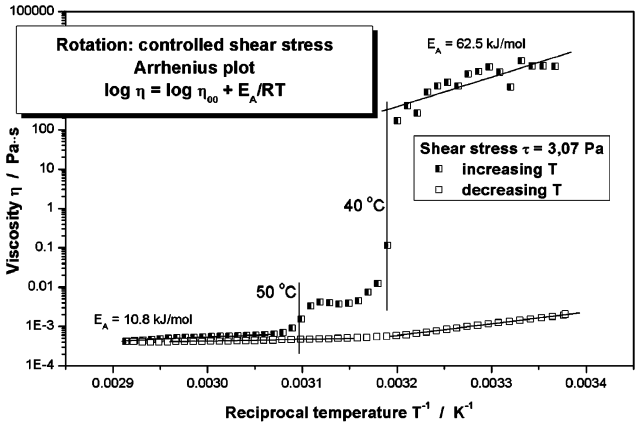

Figure 5. Dynamic viscosity, η, of PC−C32−PC (8.1 mg mL^{-1}) as a function of temperature in a controlled shear stress experiment: Arrhenius plot of log η = log η_∞ + E_A/RT.

axis in one layer. The model shown only illustrates the general principle. The resulting helix still has a large hydrophobic surface area exposed to water. To decrease this free hydrophobic surface it is likely that several helices assemble to a larger superstructure where the helices are oriented parallel to each other and form sheets.

There are some published reports assuming similar models for gel forming molecules with bulky headgroups: Fuhrhop et al. assumed that the unsymmetrical chiral bolaamphiphile N6-(12-amino-1-oxodecyl)-L-lysine takes up the same molecular arrangement with both headgroups on two different cylinders.[29] The helical strands of the monopolar dimyristoyl-5′-phosphatidyl deoxycytidine are assembled of twisted bilayers in the same manner.[44] Both molecules are chiral, so that chiral superstructures can be expected. In aqueous suspensions of the achiral [9]-10-[9]-arborol the fibers consist probably of these dumbbell-shaped molecules packed in a crossover fashion.[32] In comparison to PC−C32−PC, the arborol has a more extreme cross-section ratio between chain and headgroup, so that the molecular axes of adjacent molecules cannot form a small angle between each other. Because this angle is exactly 90°, this structure contains a plane of symmetry, so that the aggregates are achiral.

Temperature-Dependent Behavior. (a) Rheological Measurements. When aqueous samples of PC−C32−PC are heated, the viscosity drops by about 5 orders of magnitude and the gel character is lost.[38] The reason for the gel formation at low temperature is an entanglement of the stiff fibers and a possible partial parallel alignment of the fibers due to hydrophobic interactions of the exposed hydrophobic surfaces of the fibers. This entanglement and the parallel orientation can be seen in Figure 3a. Figure 5 shows the viscosity values as a function of temperature of a 8.1 mg mL^{-1} PC−C32−PC suspension for a controlled shear stress experiment. With increasing temperature, a sudden large decrease of the viscosity is observed at a temperature of 40 °C and a smaller decrease at 50 °C. The viscosity drops from 5×10^3 Pa s at room temperature to values below 5×10^{-4} Pa s at temperatures above 70 °C, i.e., values close to the viscosity of pure water at this temperature. When the sample is cooled, the viscosity shows no precipitous increase at these temperatures but only a small gradual change. Inspection of the sample shows that the formation of the gel occurs slowly

(44) Yanagawa, H.; Ogawa, Y.; Furuta, H.; Tsuno, K. *J. Am. Chem. Soc.* **1989**, *111*, 4567−4570.

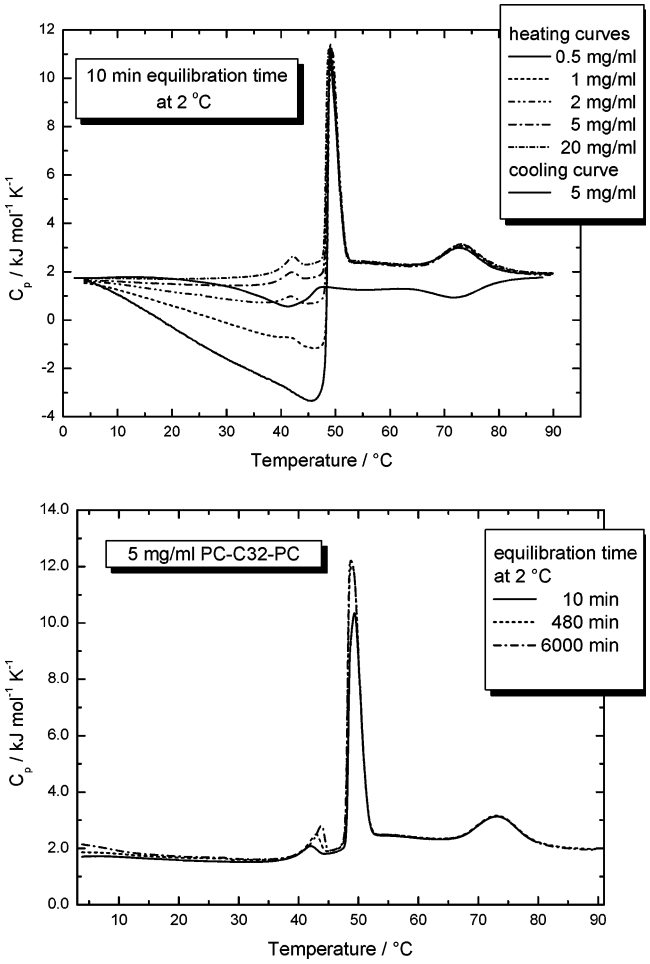

Figure 6. (Top) DSC curves for different concentrations of aqueous PC−C32−PC suspensions. (Bottom) DSC heating curves of 5 mg mL^{-1} PC−C32−PC in water after different equilibration times at 2 °C.

in diluted samples. Only when the sample is kept at room temperature for at least 1 h then the viscosity increases again drastically. The activation energy for the viscosity at low temperature, when the gel is present, is very high (62.5 kJ mol^{-1}), whereas at high temperature it is close to the activation energy for pure water (10.8 kJ mol^{-1}).

(b) DSC Measurements. To clarify the temperature-dependent behavior of PC−C32−PC suspensions in more detail and to check whether the breakdown of the gel is connected with enthalpic effects, we performed differential scanning calorimetric measurements on PC−C32−PC suspensions with different concentrations (Figure 6). The heating curves show three endothermic peaks between 5 and 90 °C. At 42 °C a pretransition with only a small transition enthalpy is observed. With increasing concentration of PC−C32−PC the transition enthalpy increases slightly. A major transition with the largest latent heat is seen at 49 °C. The molar transition enthalpy of this peak is independent from concentration. Finally, there is a very broad transition at 73 °C. This peak has the same position and the same transition enthalpy for all concentrations.

The most characteristic feature of the heating curves consists of the different slopes of the apparent molar heat capacities as a function of temperature below the main transition. The apparent molar heat capacities were calculated from the shift of the DSC curves of the sample relative to the water−water baseline assuming a partial specific volume of PC−C32−PC of 1 mL mg^{-1}.[45] All curves start at the same value of ca. 1.8 kJ mol^{-1} K^{-1}. Between 5 and 45 °C there is a strong decrease of the apparent molar heat capacity which diminishes with increasing concentration and changes into a small increase above a concentration of 5 mg mL^{-1} PC−C32−PC. For the sample with the lowest concentration, even negative apparent molar heat capacities are observed below the main transition. At the main transition a striking jump of the heat capacity to higher values, which is less pronounced at higher concentrations, can be observed. After the main transition all heating curves are on top of each other up to 90 °C and the apparent molar heat capacity has a value of 2 kJ mol^{-1} K^{-1}.

It is difficult to find an explanation for this exceptional C_p behavior. Contributions to the heat capacity can be divided into two categories.[45] The intrinsic heat capacity is determined by the degrees of freedom of molecular vibrations, rotations, motions within the lattice, the work of expansion, and their change with increasing temperature. The structural part of the heat capacity results from interactions of the bolaform molecules with the surrounding water. These interactions can be hydrophilic or hydrophobic. An increased hydrogen-bonded network around hydrophobic groups leads to a positive contribution to the heat capacity, whereas hydrophilic hydration normally leads to a decrease of C_p. It is well known that the hydrophobic effect of one CH_2 group gives a contribution of approximately 85 J mol^{-1} K^{-1}. The heat capacity of 1.8 kJ mol^{-1} K^{-1} observed at low temperature is significantly higher than the intrinsic one, which can be calculated to be about 1.2 kJ mol^{-1} K^{-1} if the chain is fluid and 0.85 kJ mol^{-1} K^{-1} if the chain is all-trans.[45] The difference of 600−950 J mol^{-1} K^{-1} corresponds to 7−11 CH_2 groups of the alkyl chain being in contact with water. Any proposed model must include this observation. As stated above for the model shown in Figure 4, the helical model leaves a large hydrophobic surface open for contact with water. This hydrophobic surface can be reduced if more than two molecules are almost parallel to each other and perpendicular to the helix axis. Another possibility to minimize the hydrophobic surface exposed to water is a tilt of the alkyl chain, i.e., an orientation deviating from 90° with respect to the helix axis. The proposed tentative model therefore is not in contradiction to the thermodynamic data.

However, the large decrease in heat capacity for the dilute samples observed in the heating cycle is difficult to explain. It is much too large to be explained by simple structural effects. Particularly for the negative values we find no explanation. The cooling curves do not show such a complicated behavior of the heat capacity but normal values as expected. In comparison to the heating curves, the enthalpic effects are smaller. The broad high-temperature transition appears again at 73 °C; the main transition shows a strong hysteresis. Instead of a sharp peak at 49 °C like in the heating curve, there is only a very broad transition at about 41 °C with a smaller enthalpy value. Thus, the reformation of a structure with higher order seems to be kinetically limited. This is consistent with the observation that it takes some time until the suspension gels after cooling from higher temperature. To check if the incomplete reformation of the fibers has an influence on the DSC heating curves, we

(45) Blume, A. *Biochemistry* **1983**, *22*, 5436−5442.

Table 1. Phase-Transition Temperatures and Molar Enthalpies of an Aqueous Suspension of 5 mg mL^{-1} PC−C32−PC after an Equilibration Time of 100 h at Low Temperature

phase transition	T (°C)	ΔH (kJ mol^{-1})
pretransition	43.8	2.7
main transition	48.7	23.2
high-temperature transition	73.0	8.0

measured thermograms of a suspension with 5 mg mL^{-1} PC−C32−PC after different annealing times at 2 °C (Figure 6). The transition at 73 °C is not influenced, but the two other peaks show a dependence on the annealing time. Whereas the temperature of the main transition remains the same, the enthalpy value increases with increasing annealing time at 2 °C. The largest effect occurs within the first 8 h. Annealing for 100 h at low temperature leads only to a very small further increase in enthalpy. The transition temperature and enthalpy of the pretransition do not reach their equilibrium values even after 8 h at 2 °C. A continuous increase in T_m and enthalpy is observed. To get reproducible data a defined cooling and heating protocol has to be carried out. The DSC curves shown in Figure 6 were obtained with 10 min of tempering at 2 °C after cooling to the starting temperature. The values for the transition temperatures and enthalpies obtained from an aqueous suspension of 5 mg mL^{-1} PC−C32−PC after an equilibration time of 100 h at 2 °C are summarized in Table 1. The sum of all transition enthalpies amounts to 34 kJ mol^{-1}. The sum of the transition enthalpies for the pre- and main transition of the phospholipid dipalmitoyl-phosphatidylcholine (DPPC) with two C_{16} chains is about 42 kJ mol^{-1} and thus slightly larger.[45] Therefore, it seems likely that the observed endothermic processes are caused in part by a chain melting process. In DPPC about 50% of the latent heat at the main transition goes into the formation of gauche conformers, another 40% is caused by a change in van der Waals interactions, and the rest due to changes in polar interactions in the headgroup region of the phospholipid.[46] We could then speculate that most of the transition enthalpy is caused by a "melting" process of the chain, i.e., the formation of gauche conformers in the alkyl chain, whereas the contribution of changes in van der Waals interactions is relatively small.

(c) FT-IR Measurements. To test our assumptions about the conformation of the PC−C32−PC molecule in the particular phases, temperature-dependent infrared spectra of a suspension with 50 mg mL^{-1} PC−C32−PC were recorded. The spectra are dominated by the CH_2 stretching and deformation vibrational bands and the symmetric PO_2^- stretching band at low wavenumber. The changes in the spectra are not readily seen in this representation. However, the wavenumber of the symmetric and antisymmetric methylene stretching vibrations $\nu(CH_2)$ provides a sensitive measure for the conformational order of the alkyl chain whereas the methylene scissoring vibration $\delta(CH_2)$ is indicative for the chain packing geometry.[47] The temperature dependence of the symmetric methylene stretching vibration is shown in Figure 7. It exhibits a characteristic two-step behavior. Below the main transition the bands at about 2869.6 and 2918.6 cm^{-1} for the symmetric and antisymmetric CH_2-stretching

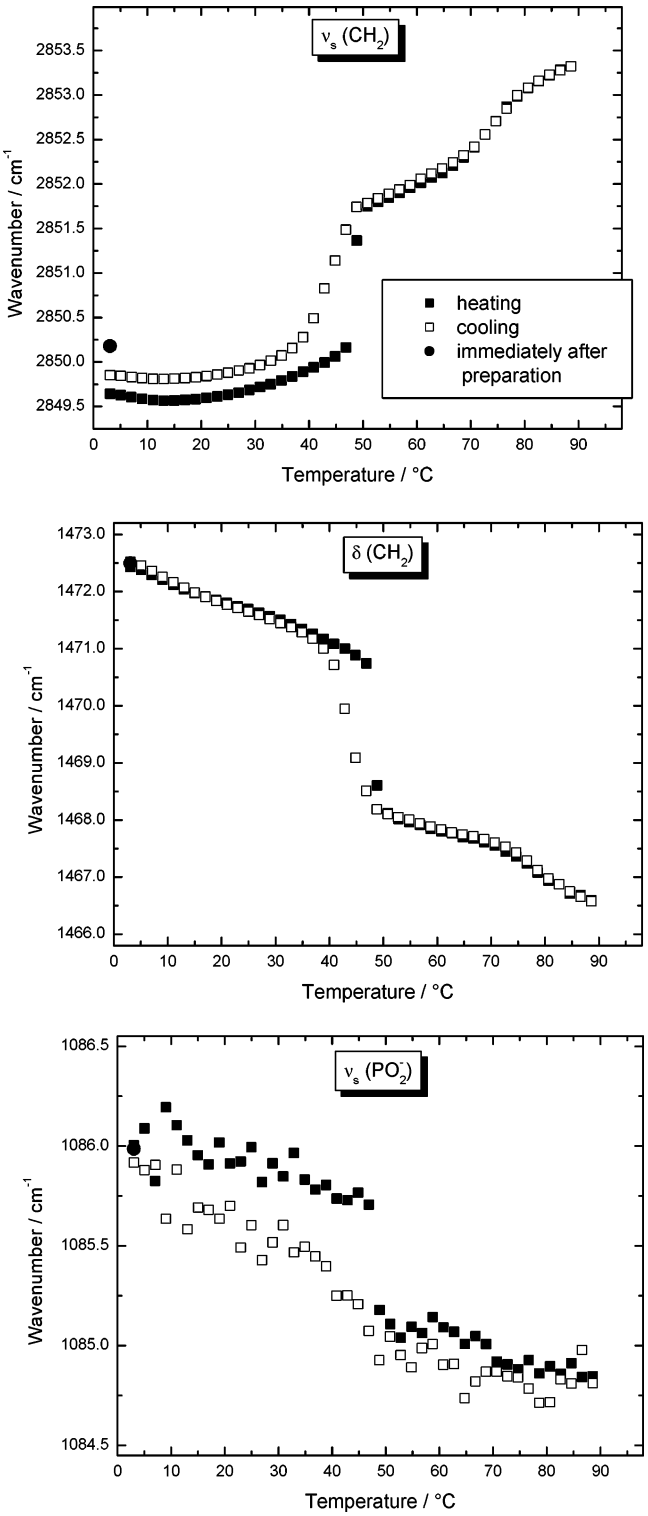

Figure 7. Wavenumbers of characteristic IR bands as a function of temperature determined for a dispersion of 50 mg mL^{-1} PC−C32−PC in D_2O and H_2O, respectively. (Top) Symmetric methylene stretching vibration. (Middle) Methylene scissoring vibration. (Bottom) Symmetric PO_2^- stretching vibration.

vibration, respectively, correspond to well-ordered extended alkyl chains in all-trans conformation, as it assumed in the model for the helix (see Figure 4). At 49 °C the bands broaden and the frequencies increase sharply. This can be attributed to a drastic decrease of the trans/gauche ratio of the C−C bonds and may be a reduced van der Waals contact of the alkyl chains.

(46) Cevc, G.; Marsch, D. *Phospholipid Bilayers. Physical Principles and Models;* Portland Press: London, 1992.
(47) Mantsch, H. H.; McElhaney, R. N. *Chem. Phys. Lipids* **1991**, *57*, 213−226.

The transition temperature agrees with the one measured with DSC for the main transition. Because we observe above the main transition no gel behavior of the solution, it is probable that smaller aggregates are present in which the molecules have an increased disorder. The high-temperature transition at 73 °C is accompanied by a further increase of the wavenumber corresponding to an additional increase of gauche conformers. This transition is broader than the main transition, as already observed before by DSC. At 90 °C bands at 2853.3 cm^{-1} for the symmetric and 2924.3 cm^{-1} for the antisymmetric methylene stretching vibration correspond to alkyl chains with a high degree of disorder, as found in the lamellar liquid-crystalline phases of phospholipids such as DPPC.[47]

In the cooling curves the high-temperature transition occurs at the same temperature as during heating, in agreement with the DSC curves. At the main transition again a hysteresis can be observed indicating a delayed reformation of the ordered structure and the fibers. In addition, at low temperatures the wavenumbers of the heating curves are not reached during cooling. Obviously the alignment of the molecules in the thermodynamically most favorable all-trans conformation is hindered and a metastable state occurs, again in agreement with the rheological and DSC data. Only after long incubation times at low temperature does the bolaform molecules reorganize and reach the state of the lowest energy. The methylene scissoring vibration shows pronounced temperature dependence as well (Figure 7). At low temperatures one observes a narrow band near 1472.5 cm^{-1} which slightly shifts with increasing temperature to lower frequencies. At the main transition a jump to 1468 cm^{-1} is seen. The high-temperature transition causes only a small further decrease of the wavenumber. This band indicates a drastic change in molecular packing and conformational order occurring at 48 °C. In the cooling cycle the starting frequency is reached again after a small hysteresis.

Whereas the CH_2 bands probe the hydrophobic alkyl chain, the phosphate PO_2^- stretching modes are useful markers for the degree of hydration of the headgroups. Since the phosphate groups of phospholipids are strongly acidic, the oxygen atoms in the moiety can only act as hydrogen-bond acceptors at neutral pH, and therefore the position of the symmetric and antisymmetric PO_2^- stretching vibrations are very sensitive to hydrogen bonding. For aqueous suspensions of PC−C32−PC, both bands are positioned at very low wavenumbers, namely, 1085 and 1220 cm^{-1}, which indicates a strong hydration of the phosphate groups. The frequency of the antisymmetric PO_2^- mode increases very slightly with increasing temperature over the whole range, indicating a decreasing number of hydrogen bonds (not shown). At the main transition the frequency decreases slightly, indicating that more water is bound to the headgroup again. A similar behavior was observed by Pohle et al. for the asymmetric bolalipid ω-hydroxybehenylphosphocholine, which forms lamellar phases however.[48] The symmetric PO_2^- stretching vibration is less sensitive for hydration effects; it decreases between 2 and 90 °C but also shows a characteristic frequency change at the main transition (see Figure 7). The FT-IR data support the DSC data and provide additional information that the conformational properties of the chain change at the main and high-temperature transition. At the main transition a hydration change of the headgroups is seen and the packing of the alkyl chain is disrupted. This all supports the previous findings that the fibers break apart at the main transition and small fiber pieces are generated which show a further decrease in size and increase in disorder at the high-temperature transition.[38]

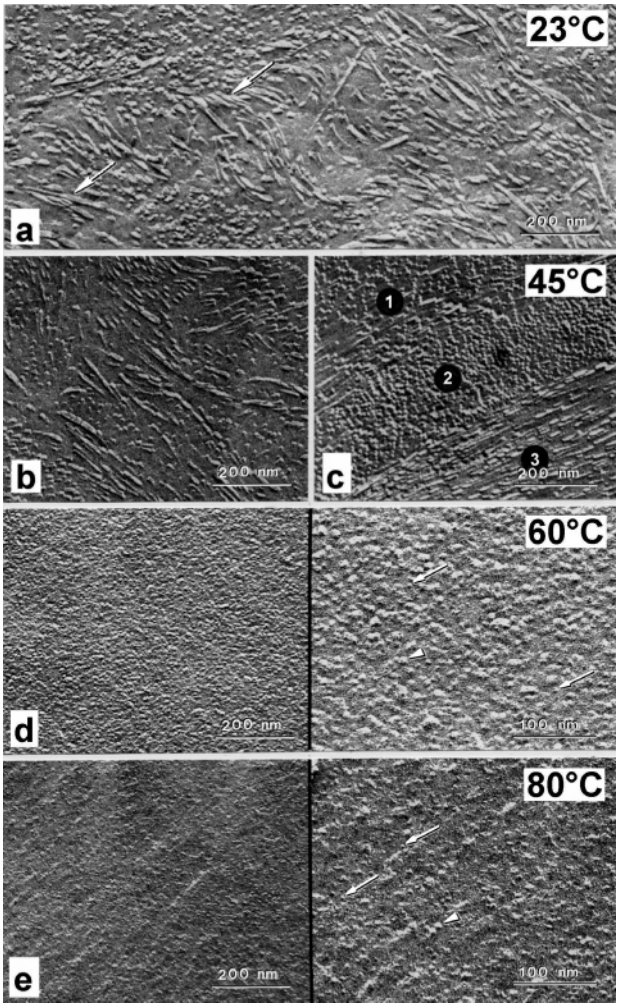

Figure 8. Freeze−fracture electron microscopic image of a suspension of 100 mg mL^{-1} PC−C32−PC in a water/glycerol mixture (4:1) quick frozen from different temperatures as indicated. The micrographs in d and e are shown in two different magnifications. See text for explanations.

(d) Freeze−Fracture Electron Microscopy. Freeze−fracture transmission electron microscopy was used to visualize the aggregate structures of the different phases below and above the main transition and the high-temperature transition. For this purpose suspensions of 100 mg mL^{-1} PC−C32−PC dispersed in a mixture of water and glycerol (4:1) were quick-frozen from different temperatures. Fracture faces of a sample frozen from room temperature show, as expected, the fibrillar structure of the hydrogel (see Figure 8). The addition of glycerol does not affect the self-assembly process of the bolaamphiphile. This was also checked by recording DSC curves in water/glycerol mixtures (not shown).

In the micrograph taken at 23 °C most of the wavy fibers with a thickness of approximately 5−7 nm run almost parallel to the fracture plane; in some areas they are slightly sticking out of the surface or are arranged in stacks (arrows in Figure 8a). In samples cooled from 45 °C, which is still below the main transition but already above the pretransition temperature,

(48) Pohle, W.; Selle, C.; Rettig, W.; Heiser, U.; Dobner, B.; Wartewig, S. *Arch. Biochem. Biophys.* **2001**, *396*, 151−161.

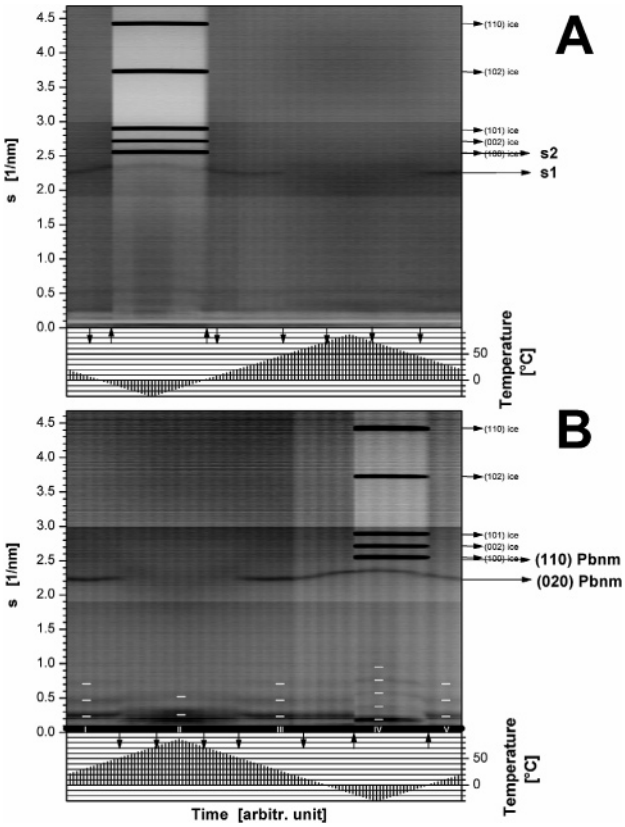

Figure 9. Contour plot of the powder diffraction pattern of a 5 wt % PC−C32−PC sample in water. (A) First cooling/heating cycle. (B) Second heating/cooling cycle of the sediment in the same capillary. White dashes mark higher order reflections with the following repeat distances: I, 4.26 nm; II, 3.85 nm; III, 4.26 nm; IV, 5.26 nm; V, 4.26 nm.

the same structure can be observed (Figure 8b). When the sample is kept at 4 °C for 4 days, heated to 45 °C, and then quenched, the freeze−fracture faces show that the fibers have oriented in parallel directions in certain areas (see Figure 8c, 1−3). The area designated with 2 shows fibers oriented almost perpendicular to the fracture plane, whereas the fibers in areas 1 and 3 are running almost parallel to the fracture plane. The fibers are less wavy than in the sample not equilibrated at 4 °C. Both suspensions quenched from 50 and 80 °C solely show smaller particles with diameters in the range of 3−10 nm (arrows and arrowheads in Figure 8d and e, right-hand side). This means that above the main transition between 48 and 73 °C as well as above the high-temperature transition similar aggregate structures exist. According to their nonuniform size they seem to consist of a variable number of molecules. The disintegration of the fibers into these particles causes the macroscopically observed breakdown of the gel. Dynamic light scattering measurements of dilute samples quenched from high temperature to 55 °C indicate the existence of small monodisperse particles having a radius of 2−5 nm and another fraction of larger aggregates.

(e) X-ray Scattering. The temperature-dependent X-ray scattering of a dilute aqueous suspension (5 mg mL^{-1} in water) of the bolaamphiphile is shown in Figure 9A as a contour plot. Our position-sensitive detector enables us to measure the scattering over the small and wide angle scattering region without an interruption of the scattering angle. Below the contour plot a graph is shown in which the cooling and heating

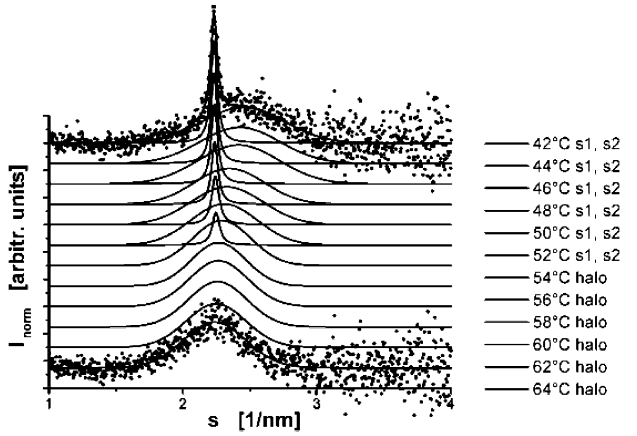

Figure 10. Fit results of the wide angle scattering in the fingerprint range. At 52 °C the halo of fluid chains disappears upon cooling and a sharp s1 on top of a broadened reflection s2 of a gel phase with a Lβ_A chain packing mode develops. The dotted curves are the experimental scattering data for two selected temperatures.

protocol is visualized. Obviously a faint but sharp reflection s1 exists in the wide angle region ($s = 2.25$ nm^{-1}, $d = 0.444$ nm). On cooling the spacing decreases continuously to $d = 0.425$ nm ($s = 2.35$ nm^{-1}) and is not affected by the appearance of the strong and sharp ice reflections. The short spacing is assigned to the lateral packing of rigid alkyl chains, which is typical of a lipid gel phase. When the sample is heated above the transition temperature (49 °C) the Bragg peak in the wide angle region disappears and only a diffuse scattering is observed. The formation of the gel phase is reversible; the wide angle peaks appear again upon cooling.

After the first cooling and heating cycle it was macroscopically observed that in the initially homogeneous sample the lipid was separated from excess water and sedimented. When the sediment in the same capillary was subjected to a further heating and cooling cycle, essentially the same behavior of the wide angle reflection is observed (Figure 9B) with the same transition temperatures. The increased scattering intensity allowed us to fit the wide angle profiles. Best results were obtained assuming the appearance of a sharp inner spacing s1 and a broad outer spacing s2 when the sample was cooled below the transition temperature (Figure 10). Furthermore, faint broad reflections in the small angle region with reciprocal spacings in the ratio 1:2:3 indicated a structure with stacked layers (Figure 9B). The X-ray scattering features imply that the sedimentation leads to aggregates and allows an estimation of the characteristic structural parameters of these aggregates. At selected temperatures the repeat distances were calculated from the small angle reflections and values of 4.26 and 3.85 nm were estimated for the gel and liquid-crystalline phases, respectively, which is small compared to the molecular length of 5.4 nm (Figure 4). Surprisingly, with the freezing of the water the repeat distance of the gel phase increased to 5.26 nm. In lyotropic lamellar phases the repeat distance is affected by the tilt angle of the chains, the headgroup conformation, and the thickness of the water layer between adjacent headgroups. When lamellar phases are subjected to lyotropic stress by the freezing of water a decrease of the repeat distance is usually observed.[49] This is interpreted by assuming the trapped water is expelled from the

(49) Förster, G.; Brezesinski, G. *Liq. Cryst.* **1989**, *5*, 1659−1668.

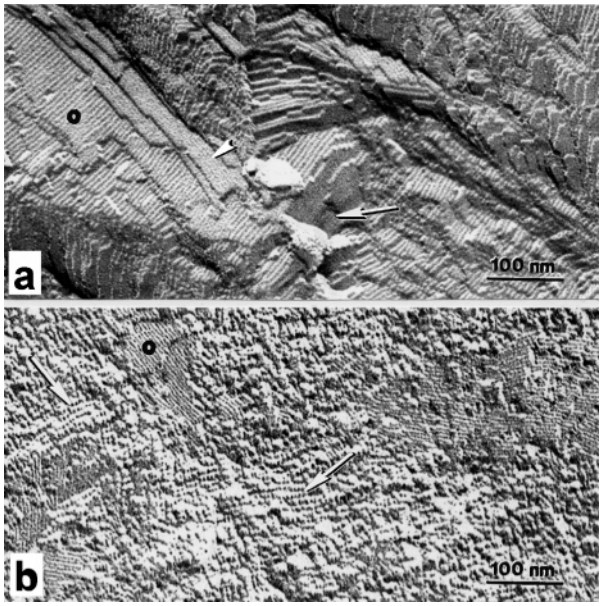

Figure 11. Freeze−fracture electron micrograph of (a) a 10 wt % PC−C32−PC sample in pure water frozen from 45 °C; arrows point to layered rows of fibers running parallel in one layer but turned by 90° in the next layers. (b) A 2 wt % sample in water frozen from 50 °C. Arrow points to fiber ends sticking out of the surface; (o) parallel fibers and layers as seen in a. The periodicities in both electron micrographs are between 5.5 and 6.5 nm.

interlamellar space during freezing. The increase in *d* observed here means that the decrease of the water layer thickness is overcompensated by a possible conformational change of the phosphatidylcholine headgroups.

The assignment of the Miller indices (020) to the short spacing s1 and (110) to s2 allows the calculation of the unit cell constants of the orthorhombic subcell (42 °C: $a = 0.458$ nm, $b = 0.897$ nm), which describes the methylene packing in the hydrocarbon layer. The observed line width of the wide angle reflections in the gel phase at room temperature support the assumption of a chain tilt when the lipids are hydrated. The sharpness of the s1 reflection as well as the appearance of the broadened s2 reflection can be explained by the model of independently scattering layers with tilted molecules, which are parallel packed but have no correlation of the molecules in the stacking direction.[50] In this case the line width of each net plane shows a characteristic value depending on the angle under which the plane is oriented to the tilting direction [100] in the subcell and on the tilt angle.

The large value of the sharp inner spacing s1 indicates a chain packing mode which is named pseudo-herringbone and included in the van der Waals energy hypersurface of orthorhombic symmetry *Pbnm* as Lβ_A.[51] It was already detected in similar unsymmetric single-chained bipolar phosphocholines[52] and in double-chained lipid systems as well.[53,54] The definite and characteristic chain packing in layers of a very diluted bolalipid suspension leads to the conclusion that both headgroups must be bent with respect to the aliphatic chain (Figure 4). Under this condition a parallel chain packing of several chains being perpendicular to the helix axis can be realized by tilting even if at each chain end a large headgroup is located.

Freeze−fracture electron micrographs of the bolalipid in water without added glycerol support the assumption of layered fibers. Figure 11 shows electron micrographs of a 100 mg mL^{-1} sample in water quenched from a temperature below the phase transition. Layered structures are clearly seen. The layers seem to consist of parallel fibers. The orientation of the fibers can change by 90° from one layer to the next. The periodicities are between 5.5 and 6.5 nm. Even if the sample is diluted, the layer structure remains in some areas of the fracture plane. In other areas the fracturing occurred perpendicular to the fiber direction and the surface shows only the fiber ends sticking out.

Conclusions

The molecular architecture of the bolaamphiphile PC−C32−PC with its two large hydrophilic headgroups connected by a long alkyl chain leads to a remarkable aggregation behavior in aqueous suspensions. Due to the large cross-sectional area of the phosphocholine headgroups compared to the smaller one of the hydrocarbon chain, the formation of a lamellar phase is very unfavorable. To reduce the interface between the hydrophobic alkyl chain surface and water, the molecules organize in a way to form fibrils with a thickness of 6−7 nm and a length of several micrometers at room temperature. Already at a concentration of 1 mg mL^{-1} the fibers form a dense network and the sample gels. A specific feature of this self-assembly process is that the hydrogelation is not induced by hydrogen bonds between the molecules, because PC−C32−PC does not possess hydrogen-bond donor atoms at neutral pH, but solely by hydrophobic interactions between the alkyl chains. Due to this fact the stability of the fibers is limited and through a temperature increase or mechanical agitation the gel structure can be broken. When the temperature is increased the fibrils collapse at a certain main transition temperature and the arrangement of the molecules changes dramatically. According to IR spectra the long chains become more disordered and TEM images show only smaller structures. In the DSC curves this transition is accompanied by an increase of the heat capacity, especially for the diluted suspensions, probably a consequence of changes at the hydrophobic/hydrophilic interface. In addition, two further phase transitions can be observed: a small pretransition at about 43 °C and a very broad high-temperature transition at 73 °C where the amount of gauche conformers within the chain increases again. At low temperatures metastable states can occur because the molecules only slowly convert into the equilibrium aggregation state of the nanofibers. This hysteresis could be observed by means of DSC as well as IR spectroscopy. Electron microscopy as well as X-ray scattering experiments show that at room temperature and higher concentration the fibers aggregate upon standing into layers with a parallel arrangements of the fibers. The surprisingly different structures observed with this bolaphospholipid are a consequence of the mismatch between the two bulky polar headgroups and the long alkyl chain. Further experiments with bolalipids modified in the headgroups as well as in the alkyl chain length are underway and will show how important the chain length

(50) Tardieu, A.; Luzatti, V.; Reman, F. C. *J. Mol. Biol.* **1973**, *75*, 711−733.
(51) Förster, G.; Meister, A.; Blume, A. *Phys. Chem. Chem. Phys.* **2000**, *2*, 4503−4508.
(52) Förster, G.; Blume, A.; Garidel, P.; Dobner, B.; Rapp, G. *Annual Report EMBL Hamburg Outstation*; Deutsches Elektronen-Synchrotron DESY: Hamburg, 2002; pp 925−926.
(53) Tenchov, B.; Koynova, R.; Rapp, G. *Biophys. J.* **2001**, *80*, 1873−1890.
(54) Tristram-Nagle, S.; Liu, Y. F.; Legleiter, J.; Nagle, J. F. *Biophys. J.* **2002**, *83*, 3324−3335.

and headgroup size will be for the formation of fibers vs micelles or lyotropic phases.

Acknowledgment. This work was supported by the Fonds der Chemischen Industrie.

Note Added after ASAP Publication. After this paper was published ASAP on November 24, 2004, errors in the temperatures in Figure 5 and the related text were corrected, and Figure 10 was replaced. The corrected version was posted December 1, 2004.

Supporting Information Available: Experimental details of the materials, sample preparation, DSC, FT-IR, TEM, rheology, X-ray scattering, and DLS. This material is available free of charge via the Internet at http://pubs.acs.org.

JA046537K